CrossMark

Process optimization and microstructure analysis in refill friction stir spot welding of 3-mm-thick Al-Mg-Si aluminum alloy

L. M. Santana[1,2] · U.F.H. Suhuddin[1] · M. H. Ölscher[3] · T. R. Strohaecker[2] ·
J. F. dos Santos[1]

Abstract Novel ultra-high-strength aluminum alloys provide enormous lightweighting potential for modern car body design. However, joining such alloys can be challenging. Refill friction stir spot welding is a solid-state joining process that provides fundamental advantages compared to conventional joining technologies when welding aluminum alloys. This work presents refill friction stir spot welding for joining 3-mm-thick Al-Mg-Si alloys. The welded joints have been optimized for shear load condition by the design of experiment and analysis of variance. The results show that it is possible to obtain welds of relatively thick Al-Mg-Si alloys with good mechanical properties. Microstructure analyses show that rotational speed and plunge depth play important roles in the bonded width and hook height, which affect the mechanical performance of the joint.

Highlights • Friction spot welding of Al-Si-Mg alloy single-lap joints was demonstrated.
• The influence of joining parameters on joint mechanical performance was determined.
• A mathematical model for estimating lap shear strength was successfully established.

✉ U.F.H. Suhuddin
   uceu.suhuddin@hzg.de

1   Institute of Materials Research, Materials Mechanics, Solid State Joining Processes, Helmholtz-ZentrumGeesthacht GmbH, Geesthacht, Germany

2   Metallurgical Engineering Department, Federal University of Rio Grande do Sul, Porto Alegre, Brazil

3   Ford Werke GmbH,Ford Research and Advance Engineering,Advanced Materials and Processes, Aachen, Germany

1 Introduction

Automakers continuously put efforts to develop new technologies that lead to reduced fuel consumption. Lightweighting is one of several means to reduce CO_2 emissions and comply with current and future environmental legislation [1]. Currently, lightweight materials such as aluminum are extensively used even in the high-volume vehicle segment. The trend in the aluminum industry is towards higher strength aluminum alloys that enable enhanced lightweight designs [2]. However, the integration of such materials in a high-volume vehicle is challenging due to the lack of suitable joining technologies. Well-established processes such as resistance spot welding or self-pierce riveting are at their limits when joining novel lightweight materials that are high in strength but limited in ductility paired with severe hot crack sensitivity.
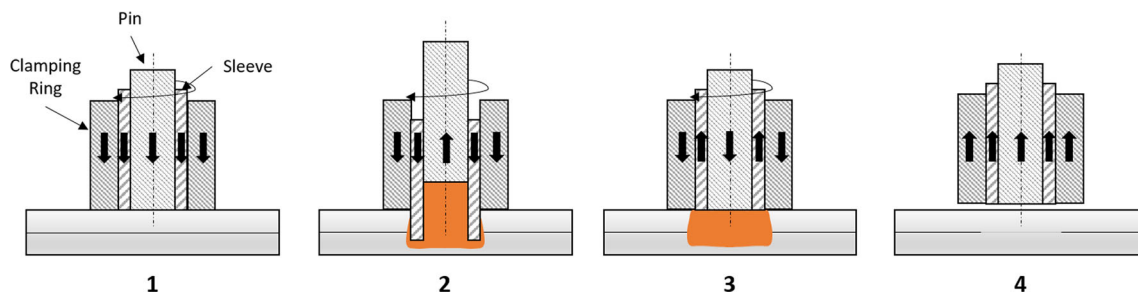
Refill friction stir spot welding (refill FSSW), also known as friction spot welding (FSpW), is a solid-state joining process able to bypass many of the existing challenges related to the joining of high-strength aluminum alloys. Refill FSSW uses a non-consumable tool consisting of a stationary clamping ring, rotating pin, and sleeve [3–19]. The sleeve plunge process variant is presented in Fig. 1. In the first stage, the upper and lower parts are held together by the clamping ring and the backing anvil. Simultaneously, the sleeve and pin start to rotate. In the second stage, the rotating sleeve plunges into the materials while the rotating pin is moved in the opposite direction. The tool introduces plastic deformation and generates frictional heat to plasticize the materials. The

Fig. 1 Illustration of refill FSSW process using sleeve plunge variant: (*1*) Clamping and tool rotation. (*2*) Sleeve plunge and pin retraction. (*3*) Sleeve and pin return to surface level. (*4*) Tool removal

softened material is squeezed into a cavity left by the pin. Then, the rotating sleeve and pin return to their initial position, forcing the plasticized metal to refill the welded area. In the last step, the tool is retracted, leaving a joint without a keyhole. Refill FSSW is an automatable process in which the tool head can be adapted to a C-frame weld gun. This joining process does not increase the weight of the structure because no additional fastener or rivet is used. Compared to conventional fusion welding processes, refill FSSW consumes less energy and produces joints with a good surface finish [4, 5].

Some published works [5–15] have reported that refill FSSW has been successfully used to weld relatively thin materials, up to 2 mm thick, in similar and dissimilar joint combinations with good mechanical properties. In similar joint configuration, the weld strength of the joint is driven by a geometrical feature, denominated hook, and the extension of the welded area [6, 7]. The hook is defined as a partially bonded region and is a transition from the unbonded interface separating the overlapped plates to the fully metallurgically bonded region. During loading, the hook acts as a stress concentrator and provides a potential path for crack initiation and propagation [16]. The formation of the hook is induced by tool movement during plunging/retracting and is associated with the welding parameters [7]. Refill FSSW in similar 2-mm-thick AZ31 Mg alloys showed that both the hook height and the welded area affect the weld strength. An increase in the weld strength is initially observed as the welded area becomes larger. However, the hook has a greater influence at greater size, which then overrides the benefits of having a large welded area [16]. However, the formation of the joint

microstructure, which also affects the weld strength, is governed by welding parameters and has not been fully understood yet.

The objective of this work is to establish a parameter range leading to high weld strength for the refill FSSW of 3-mm-thick Al-Mg-Si alloy by utilizing the design of experiments (DOE). Analysis of variance (ANOVA) and response surface methodology (RSM) are used to systematically investigate the influence of welding parameters on the mechanical performance of the welds. An attempt is made to understand the microstructure of the welded area and to correlate the microstructure with the strength of the joints.

2 Experimental procedure

The alloy used in this study is a heat-treatable Al-Mg-Si wrought alloy. Coupons with dimensions of 100 × 25.4 × 3 mm were

Table 2 Welding combination according to Box–Behnken design

Combination	Rotational speed (rpm)	Plunge depth (mm)	Retracting rate (mm/s)
1	1800	3	3.5
2	3000	3	3.5
3	1800	3.8	3.5
4	3000	3.8	3.5
5	1800	3.4	2.5
6	3000	3.4	2.5
7	1800	3.4	4.5
8	3000	3.4	4.5
9	2400	3	2.5
10	2400	3.8	2.5
11	2400	3	4.5
12	2400	3.8	4.5
13	2400	3.4	3.5
14	2400	3.4	3.5
15	2400	3.4	3.5
16	2400	3.4	3.5
17	2400	3.4	3.5

Table 1 FSpW process parameters and levels

Symbol	Welding parameter	Unit	Levels		
			−1	0	1
RS	Rotational speed	rpm	1800	2400	3000
PD	Plunge depth	mm	3.0	3.4	3.8
RR	Retraction rate	mm/s	2.5	3.5	4.5

Table 3 ANOVA of LSS values

Source	SS	df	MS	F value	p value	Contrib. [%]
RS (rpm)	6.125	1	6.125	33.88	0.001	36.6
PD (mm)	2.162	1	2.16201	11.96	0.011	12.9
RR (mm/s)	0.3195	1	0.31954	1.77	0.225	1.9
RS^2	0.1546	1	0.15464	0.86	0.386	0.9
PD^2	1.9547	1	1.95473	10.81	0.013	11.7
RR^2	0.0002	1	0.00017	0	0.976	0.0
RS × PD	2.7889	1	2.7889	15.43	0.006	16.7
RS × RR	1.1236	1	1.1236	6.22	0.041	6.7
PD × RR	0.7734	1	0.7734	4.28	0.077	4.6
Error	1.2654	7	0.18077			7.6
Total	16.7439	16				

used in this work. Prior to joining, the parts were cleaned with acetone to remove surface contamination.

Single overlap joints were made using a RPS 100 friction spot welding machine and tool with diameters of 17, 9, and 6 mm for the clamping ring, sleeve, and pin, respectively. Lap shear testing was performed to evaluate the mechanical performance of the joints using a Zwick–Roell model 1478 universal testing machine with a crosshead speed of 2 mm/min at room temperature.

DOE is an advantageous method for determining the effect of the factors on the output of the process. It includes the process of planning, designing, and analyzing the experiment so that valid and objective conclusions can be drawn effectively and efficiently [20]. A Box–Behnken design (BBD) with three factors, rotational speed (RS), plunge depth (PD), and retracting rate (RR), was selected to evaluate the weld strength. Table 1 compiles the process parameters and levels used in this work. The range of welding parameters (levels), as the input for BBD experiments, was selected based on preliminary studies. No dwell time was used in this process. The plunging rate and clamping force were kept constant at 4 mm/s and 13 kN, respectively.

ANOVA was used to evaluate the influence of the selected parameters and their interactions on the mechanical performance of the joint. RSM was applied to better understand the mechanical performance responses with the variation of the weld parameters and to optimize the welding parameters to achieve the maximum strength.

The microstructures of the joints were analyzed by optical microscopy to understand the interactions among the process parameters, microstructure, and mechanical performance. The samples were cross-sectioned, ground, polished, and electrically etched in Barker etchant (5 vol% fluoroboric acid in water) for observation under polarized light.

3 Results and discussion

3.1 Design of experiment and analysis of variance

The BBD test matrix used in the current study is shown in Table 2.

Table 3 shows the ANOVA of the acquired data with a confidence interval of 95%. According to the results, RS, PD, and PD^2, and the interactions RS × PD and RS × RR are significant factors affecting the mechanical performance of the joints. The contribution of each factor to the total variation can be written in terms of percentage, dividing the sum of squares (SS) of each factor by the total SS of the experiment. The factors are considered physically significant if the percentage of contribution is higher than the associated error. RS was shown to be the major parameter affecting the lap shear strength (LSS) of the joints (36.6%), followed by the interaction RS × PD (16.7%) and PD (12.9%). Meanwhile, RR seems to have no significant influence on the LSS response for the selected welding parameter range.

Figure 2 shows the main effects plot for mean LSS. The horizontal dashed lines show the value of the total mean of LSS. RS clearly has the highest influence on LSS, in which an

**Fig. 2** Main effect plots of RS (**a**), PD (**b**), and RR (**c**)
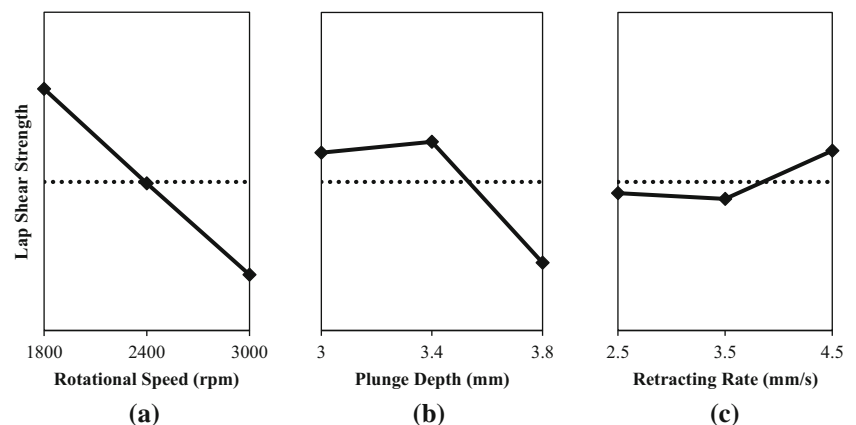
Fig. 3 Effects of the interactions between *RS* (rotational speed), *PD* (plunge depth), and *RR* (retracting rate) on the mean LSS
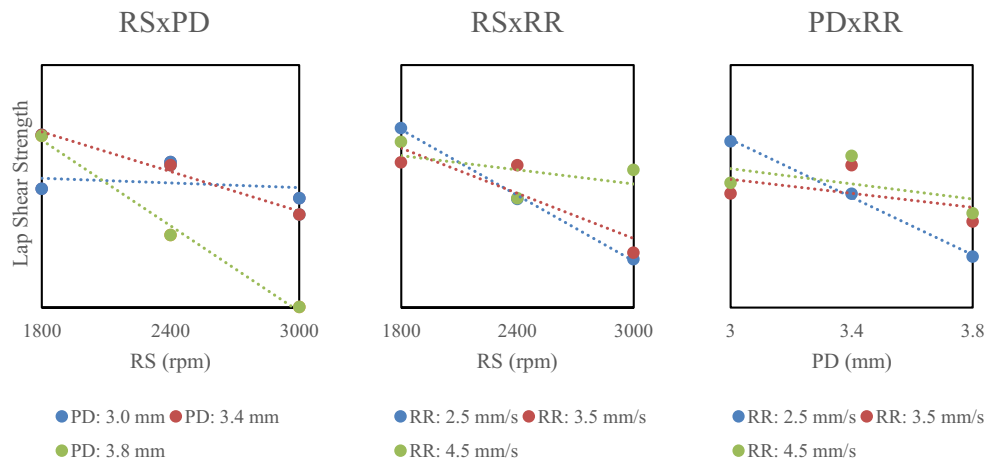

increase in RS leads to a decrease in LSS. PD appears to show a quadratic behavior where the LSS reaches a maximum at approximately 3.4 mm. Additionally, it should be noted that the increase in RR leads to an increase in LSS, although its effect on LSS is not as significant as the effect of RS and PD.

To better understand the influence of the interactions of the welding parameters in two-way combinations on the mean LSS, the two-dimensional interaction plot is presented in Fig. 3. Because there are no parallel interaction lines in the interaction plot of RS × PD and RS × RR, these interactions
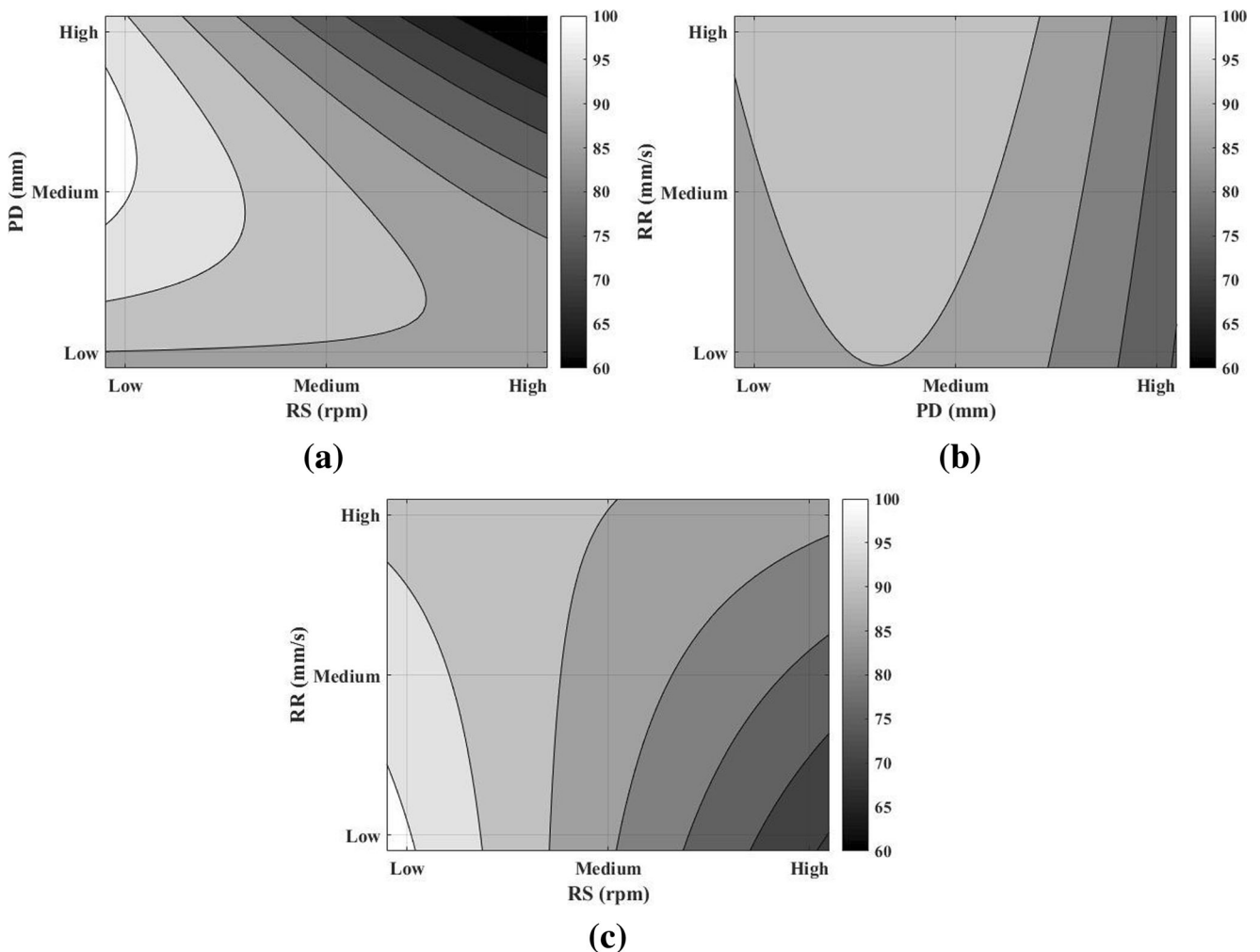
Fig. 4 Contour plots of LSS in percentage as function of welding parameters. PD vs RD (**a**), RR vs PD (**b**), and RR vs RS (**c**)
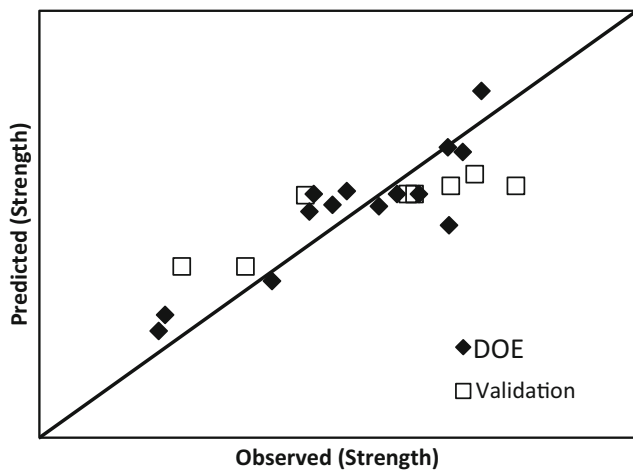
Fig. 5 Comparison of predicted LSS according to Eq. 1 and experimental data

are considered to affect the mechanical performance of the joint. The effects of the welding parameters and their interaction on the mechanical performance of the joint are in agreement with some previous studies on the refill FSSW of Al alloys [6–8, 15].

3.2 Response surface methodology

Based on the results obtained from the BBD, a regression model for LSS prediction was developed including only the significant welding parameters. Notwithstanding the low contribution of to the LSS, it should be considered in the function for hierarchical reasons, as the interaction RS × RR makes a significant contribution to LSS.

$$LSS = f(RS, PD, RR) = -54.9 + 0.00728 \times RS + 36.48$$

$$\times PP - 1.92 \times RR - 4.33 \times PD^2 - \tag{1}$$

$$0.003479 \times RS \times PD + 0.0008833 \times RS \times RR$$

Equation (1) is depicted as two-dimensional contour plots in Fig. 4. Each plot represents the effect of two welding parameters on LSS, in which the third parameter is kept constant at the center point of 3.5 mm/s for RR, 2400 rpm for RS, and 3.4 mm for PD in Fig. 4a–c, respectively. The highest values of LSS are reached at intermediate levels of PD and low RS. Increasing RR tends to increase LSS, but the effect is less evident.

Eight additional confirmation experiments were conducted with new process parameters chosen within the range from which the equation was derived to verify the adequacy of the developed model. They are depicted in the graph as white rectangles in Fig. 5. The error in the predicted LSS varies from 10.4 to 11.4%, which is consistent with the coefficient of determination (R^2) of

Fig. 6 Cross-section of a typical joint and characteristic zones. Low-magnification overview (**a**), base material (**b**), stir zone (**c**), thermo-mechanically affected zone (**d**), and hook (**e**)
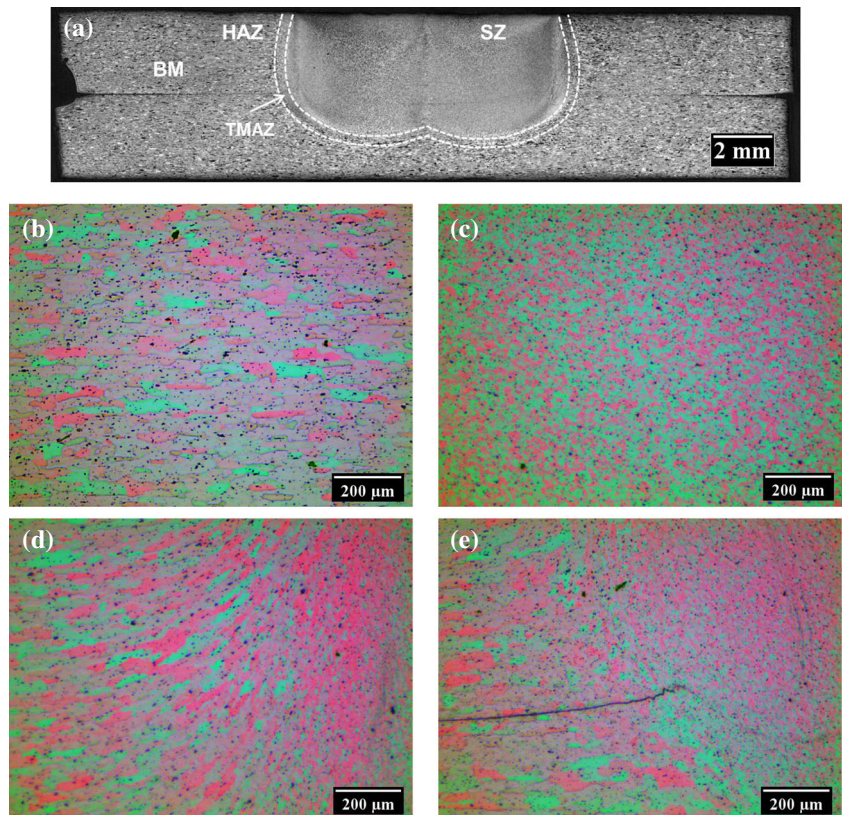
Fig. 7 Schematic illustration of the dimensional measurements of the bonded width and hook
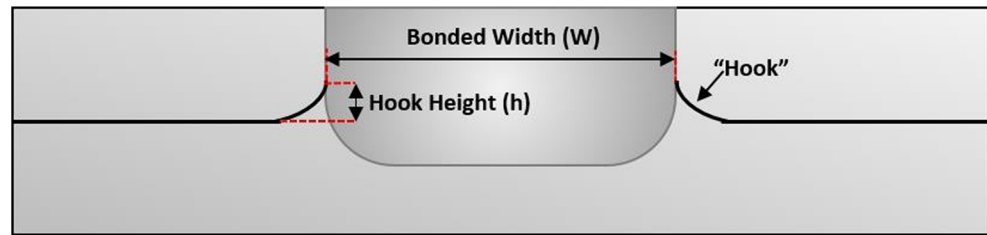
approximately 0.87. It is possible to see the satisfactory agreement between the model and the observed values by analyzing the plot of the predicted versus observed values.

3.3 Microstructure evaluation

Figure 6a presents a typical micrograph of the weld cross-section. No defects or obvious thickness reduction were observed in the weld. Based on grain structure, the welded area is characterized into two zones: the stir zone (SZ), the thermo-mechanically affected zone (TMAZ), and the base material (BM).

The BM (Fig. 6b) consists of an elongated grain structure. The SZ is characterized by fine grain structure due to dynamic recrystallization [4, 9, 16, 21]. This region underwent severe plastic deformation due to the sleeve and pin movement and was exposed to high temperature, as illustrated in Fig. 6c. The TMAZ (Fig. 6d) consists of deformed grains affected by less intense plastic deformation and thermal exposure than in the SZ.

An additional microstructure feature that is important for the mechanical performance in the similar joint configuration is the hook [7, 16, 21]. The hook is formed at the transition between the unwelded sheet interface and the metallurgically bonded region. It is formed by the upward bending of the sheet interface due to tool movement during penetration and retraction. A typical hook pattern is presented in Fig. 6e, located at the border of the TMAZ and SZ.

To clarify how the relationship between the LSS and the microstructure affects the mechanical performance, the bonded width (W) and hook height (h) were measured as shown in Fig. 7.

The effects of the hook height and the bonding width on the LSS are shown in Fig. 8. An increase in h leads to a decrease in LSS, whereas an increase in W will increase LSS up to a maximum, before it decreases again. Thus, when the hook height is not obvious, the bonded width plays an important role in the mechanical performance. However, when the height of the hook is greater than a certain threshold, it will override the beneficial effect of the bonded width and become the dominant factor affecting the LSS.

To obtain a better understanding of the effects of RS and PD on mechanical performance as obtained from the ANOVA (Table 3), the microstructures of the welds produced by different welding parameters are discussed.

Fig. 9 compares the microstructures of welds produced by a low RS of 1800 rpm and a high RS of 3000 rpm with the same PD of 3.8 mm and RR of 3.5 mm/s. It should be noted that the tool plunges through the upper sheet into the lower sheet in both welds. It is possible to observe a greater hook height in the microstructure of the weld performed with higher RS. Additionally, the two welds have distinct grain morphology in the TMAZ. In the weld with higher RS, the elongated grains of the TMAZ are clearly bent up, parallel to the hook shape. In contrast, the weld with lower RS has a finer grain in the TMAZ, most likely due to dynamic recrystallization during the process. It is well known that the tip of the hook acts as a

Fig. 8 Effect of hook geometry on lap shear strength. Hook height (**a**) and bonded width (**b**)
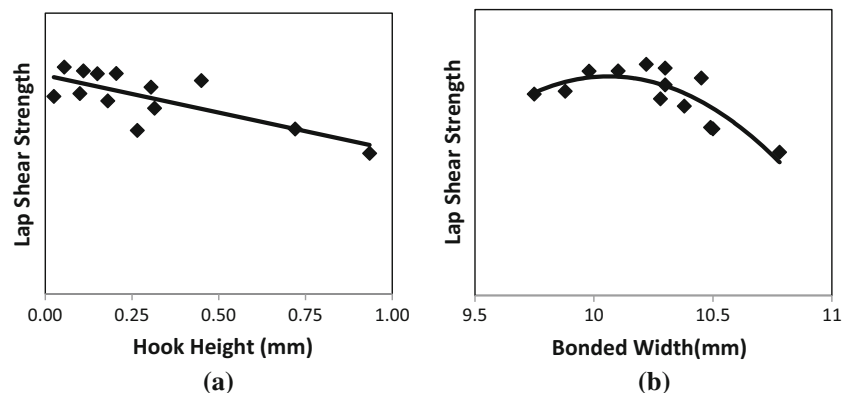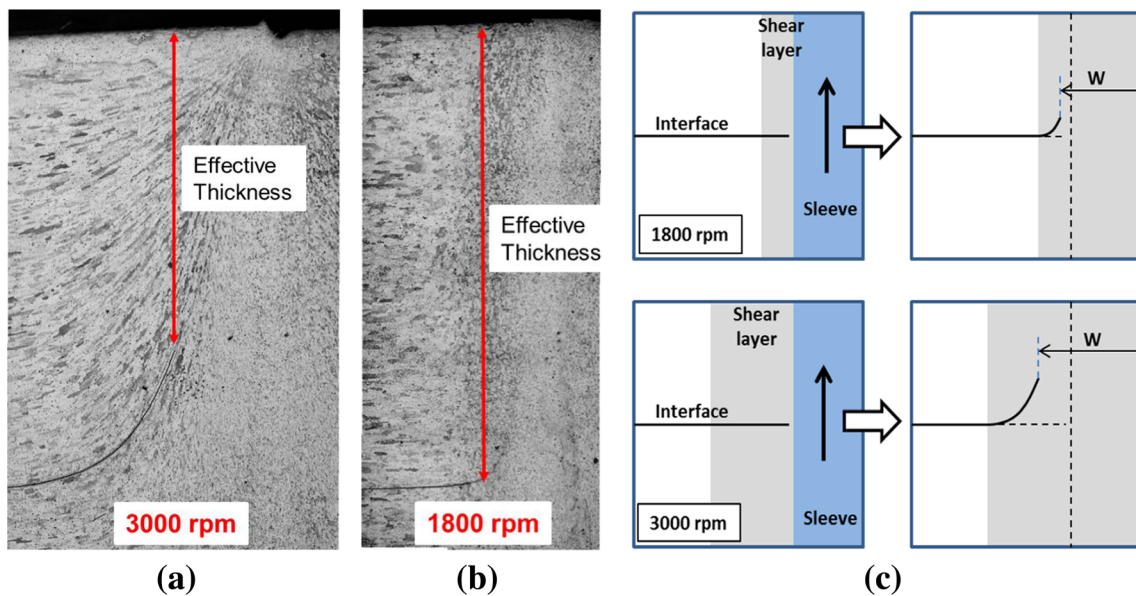
Fig. 9 Detail of the hook zone of a joint welded with low RS (**a**), a joint welded with high RS (**b**), and the schematic illustration of hook formation (**c**)

stress concentrator, in which failure initiates [6, 16]. Therefore, the weld with larger effective thickness and fine grains beyond the hook tip has better mechanical properties than the weld with lower effective thickness and elongated grains. This observation is in good agreement with some previous studies [6, 15, 16] showing that the hook geometry plays an important role in mechanical performance. It is believed that the bonded width and hook height are driven by the shear layer. An increase in RS will cause a higher heat input, which then plasticizes a larger amount of material near the tool. During sleeve retraction, the sleeve will deform a larger area at the interface in the higher heat input welding parameter; in other words, it has a larger shear layer resulting in a larger welded area and higher hook, as illustrated in Fig. 9c.

The microstructures of the welds produced by different PDs of 3.0 and 3.8 mm with the same RS of 2400 rpm and RR of 2.5 mm/s are depicted in Fig. 10. It can be seen that an elevated vertical hook is observed for the deeper PD. The deeper PD means also slightly longer welding time, which results in higher heat input and also extended deformation

(material flow). Therefore, during retraction, the sleeve movement produces a larger shear layer and introduces more upward material flow for the deeper PD.

4 Conclusions

In this study, refill FSSW was used to weld 3-mm-thick Al-Mg-Si alloy. Based on the experimental and analytical results, the following conclusions can be drawn.

- BBD experiments were sFord Werke GmbH,Ford Research and Advance Engineering,Advanced Materials and Processesuccessfully conducted to define a welding parameter range to weld relatively thick Al-Mg-Si alloy with good mechanical performance.
- Based on analysis of variance, RS was the factor with the largest influence on the LSS of the joints (36.6%), followed by the interaction of RS × PD (16.7%) and then PD (12.9%).

Fig. 10 Detail of the hook zone of a joint welded with low PD (**a**) and a joint welded with high PD (**b**)
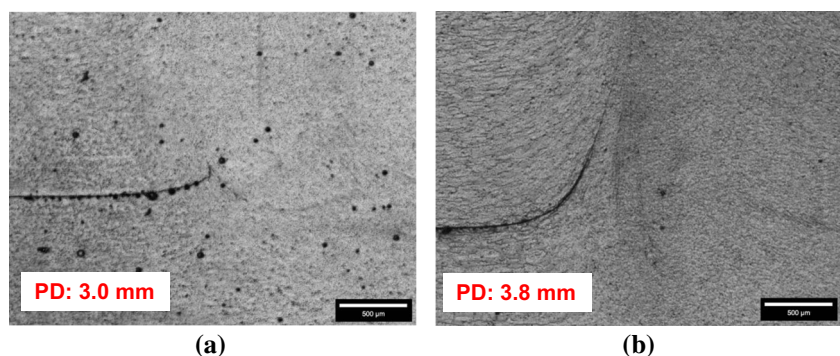
- RSM was used to develop a mathematical model for predicting LSS as a function of RS, PD, and RR. The verifications indicated adequate agreement between the predicted and experimental values.

- Microstructure analyses revealed that the hook height and welded area play fundamental roles in the mechanical strength of the welds. The bonded width plays an important role in the mechanical performance when the hook height is not obvious. However, the hook will override the effect of the bonded width and become the dominant factor affecting the LSS when its height exceeds a certain threshold.

- The formation of the hook and the bonded width are affected by the shear layer, which is induced by the welding parameters.

References

1. T. Skszek, M. Zaluzec, J. Conklin, D. Wagner (2015) MMLV: project overview, SAE technical paper 2015–01-0407. doi: 10.4271/2015-01-0407.

2. C. A. Graf (2015) Automotive Circle Insight Edition @ Ford USA.

3. Schilling CDS, dos Santos JF (2004) Method and device for joining at least two adjoining work pieces by friction welding. GKSS Forschungszentrum Geesthacht Gmbh, United States Patent, US.

4. Amancio-Filho ST, Camillo APC, Bergmann L et al (2011) Preliminary investigation of the microstructure and mechanical behaviour of 2024 aluminium alloy friction spot welds. Mater Trans 52:985–991. doi:10.2320/matertrans.L-MZ201126

5. Shen Z, Yang X, Yang S, Zhang Z et al (2014) Microstructure and mechanical properties of friction spot welded 6061-T4 aluminum alloy. Mater Des 54(2014):766–778. doi:10.1016/j.matdes.2013.08.021

6. Rosendo T, Parra B, Tier MAD et al (2011) Mechanical and microstructural investigation of friction spot welded AA6181-T4 aluminium alloy. Mater Des 32:1094–1100. doi:10.1016/j.matdes.2010.11.017

7. Cao JY, Wang M, Kong L et al (2016) Hook formation and mechanical properties of friction spot welding in alloy 6061-T6. J Mater Process Technol 230:254–262. doi:10.1016/j.jmatprotec.2015.11.026

8. Zhao YQ, Liu HJ, Chen SX et al (2014) Effects of sleeve plunge depth on microstructures and mechanical properties of friction spot welded alclad 7B04-T74 aluminum alloy. Mater Des 62:40–46. doi:10.1016/j.jmatprotec.2015.11.026

9. Tier MD, Rosendo TS, dos Santos JF et al (2013) The influence of refill FSSW parameters on the microstructure and shear strength of 5042 aluminium welds. J Mater Process Technol 213:997–1005. doi:10.1016/j.jmatprotec.2012.12.009

10. Effertz PS, Infante V, Quintino L et al (2016) Fatigue life assessment of friction spot welded 7050-T76 aluminium alloy using Weibull distribution. Inter J Fatigue 87:381–390. doi:10.1016/j.ijfatigue.2016.02.030

11. Campanelli LC, Suhuddin UFH, dos Santos JF et al (2012) Preliminary investigation on friction spot welding of AZ31 magnesium alloy. Mater Sci Forum 706-709:3016–3021. doi:10.4028/www.scientific.net/MSF.706-709.3016

12. Plaine AH, Gonzalez AR, Suhuddin UFH et al (2015) The optimization of friction spot welding process parameters in AA6181-T4 and Ti6Al4V dissimilar joints. Mater Des 83:36–41. doi:10.1016/j.matdes.2015.05.082

13. Shen J, Suhuddin UFH, Cardillo MEB et al (2014) Eutectic structures in friction spot welding joint of aluminum alloy to copper. Appl Phys Lett 104:191901. doi:10.1063/1.4876238

14. Suhuddin U, Fischer V, Kroeff F et al (2014) Microstructure and mechanical properties of friction spot welds of dissimilar AA5754 Al and AZ31 Mg alloys. Mater Sci Eng A 590:384–389. doi:10.1016/j.msea.2013.10.057

15. Pieta G, dos Santos JF, Strohaecker TR et al (2014) Optimization of friction spot welding process parameters for AA2198-T8 sheets. Mater Manuf Process 29:934–940. doi:10.1080/10426914.2013.811727

16. Campanelli LC, Suhuddin UFH, Antonialli AÍS et al (2013) Metallurgy and mechanical performance of AZ31 magnesium alloy friction spot welds. J Mater Process Technol 213:515–521. doi:10.1016/j.jmatprotec.2012.11.002

17. Zhao Y, Liu H, Yang T et al (2016) Study of temperature and material flow during friction spot welding of 7B04-T74 aluminum alloy. Int J Adv Manuf Technol 83:1467–1475. doi:10.1007/s00170-015-7681-2

18. Plaine AH, Gonzalez AR, Suhuddin UFH et al (2016) Process parameter optimization in friction spot welding of AA5754 and Ti6Al4V dissimilar joints using response surface methodology. Int J Adv Manuf Technol 85:1575–1583. doi:10.1007/s00170-015-8055-5

19. Ji S, Wang Y, Zhang J et al (2017) Influence of rotating speed on microstructure and peel strength of friction spot welded 2024-T4 aluminum alloy. Int J Adv Manuf Technol 90:717–723. doi:10.1007/s00170-016-9398-2

20. Montgomery DC (2000) Design and analysis of experiments. Wiley, New York

21. Yin YH, Sun N, North TH et al (2010) Hook formation and mechanical properties in AZ31 friction stir spot welds. J Mater Process Technol 210:2062–2070. doi:10.1016/j.jmatprotec.2010.07.029